Characterisation methods for functionally graded materials

G. TOMANDL*, M. MANGLER
Institute of Ceramic Materials, Gustav-Zeuner Str. 3, D-09596 Freiberg, Germany
E-mail: tomandl@ikw.tu-freiberg.de

D. STOYAN, A. TSCHESCHEL
Institute of Stochastics, Agricolastr. 1, D-09595 Freiberg, Germany

TU BERGAKADEMIE FREIBERG
Institute of Ceramic Materials, Gustav-Zeuner Str. 3, D-09596 Freiberg, Germany

J. GOEBBELS, G. WEIDEMANN
Federal Institute for Materials Research and Testing, Unter den Eichen 87, D-12205 Berlin, Germany

Published online: 13 June 2006

In this paper the characterisation of functionally graded materials is elucidated by several different methods. These methods described here are used for the quantitative analysis of materials with a local dependence of microstructure parameters. Using X-ray microscopy (computed tomography) for 3D-measurements and optical microscopy on polished sections for 1D and 2D measurements on the same sample, a ceramic filter consisting of sintered spherical particles, various mathematical evaluation methods are described and compared.

1. Introduction

The development of new materials with structural gradients requires new methods to characterise their microstructure and to determine the properties of these materials.

Traditional statistical image analysis of gradient structures is based on series of measuring fields, which is only able to detect small gradients, e.g. [1–3]. This paper represents methods for the analysis of steep gradients within a single image, based on cross-section preparation of materials. One particular aim is the determination of the location-dependent pore size distribution in thin ceramic layers with pore sizes down to the nanometer scale (e.g. in ceramic membranes) [4].

For this task, both particle size and pore size distributions, for most of the functional gradient materials (FGM) a direct determination of the spatial microstructural parameters is most often not possible. An exception is the computed tomography (CT), however, in most cases not with sufficient resolution (about 2 μm). Therefore, methods had to be developed by evaluating area-(2D) or linear (1D) data on planar sections to determine the local dependence of the spatial parameters (3D).

In order to compare these 1D- and 2D-methods with the 3D-evaluation method (CT) a ceramic filter was selected, which was prepared by vibration densification of layers of Al_2O_3-particles with diameters >1 mm, sintered at 1700°C.

In this paper two experimental methods (conputed tomography and image analysis on polished sections), and three new mathematical methods (i) calculating the position dependence of the equivalent sphere diameter frequency distribution from the local dependence of the equivalent circle diameter or the chord length frequency distributions; (ii) describing the gradient of the porosity by mathematical morphology, based on 3D-data, obtained with CT) are shown.

2. Computed tomography

Computed tomography (CT) is the only non-invasive evaluation method to analyse three-dimensional density gradients. The result of a CT measurement is usually given

*Author to whom all correspondence should be addressed.
0022-2461
DOI: 10.1007/s10853-006-6632-6

in form of a 3D image matrix. Each point represents a single volume element, a voxel. CT delivers an absolute measure, the linear attenuation coefficient μ, for the absorbed X-ray radiation averaged over one voxel.

For high resolution tomography an X-ray source with a small focal spot is desirable. X-ray tubes with transmission target allow for focal spot sizes down to microns. High resolution in the object plane is reached by magnification technique. X-ray cone beam geometry leads to a 3D image of the whole object. Special cone beam algorithms are developed for the image reconstruction. The most common used formalism is the Feldkamp [5] algorithm. The high resolution tomograph, developed at BAM[1], works with a 100 kV transmission target X-ray tube and a CCD camera cooled to improve the signal-to-noise ratio. The scintillator is a thin GdOS (Gadolinium Oxysulphide) layer deposited on the fibre taper.

Two important features characterising the system performance of a tomographic apparatus are the spatial resolution and the contrast or density resolution. With a pixel size of $(1.1\ \mu\text{m})^3$ the spatial resolution is about 320 Lp/mm (line pairs/mm) corresponding to about 1.5 μm. The best standard deviation σ of the contrast resolution was about $\Delta\mu/\mu = 4.8\%$ [6].

First gradient samples studied by CT were samples (Cu-Fe and Cu-W system, TU Dresden [7]) prepared by centrifugal powder forming in the green state (embedded in epoxy) to examine the three-dimensional gradient in the composition. Differences in the attenuation coefficient could be characterised together with some details like spots with a higher density [8].

For the present investigations the ceramic filter was used as described above. The sample consists of five layers of Al_2O_3 spheres (five size fractions $D = 1.6$–2.0, 2.0–2.5, 2.5–3.15, 3.15–3.5, 3.5–4.5 mm) sintered together giving a gradient in the diameter from top to bottom of the sample. Fig. 1 shows an isosurface representation of the sample. A three-dimensional algorithm was developed to identify each sphere and to provide information about its size and position. The plot of the total frequency distribution of sphere diameters shows clearly four separated peaks (Fig. 2). The peak from 2.8 to 3.8 mm is quite broad and suggests the existence of two overlapping peaks. This idea is supported by the locally resolved points in the same figure, which shows one sharp peak at a horizontal position of about 35 mm and a sphere diameter of about 3.4 mm which overlaps with a broad peak of smaller spheres which occur at horizontal positions ranging from 10 to 40 mm and having sphere diameters ranging from 2.8 to 3.4 mm. For comparison in section 3 (Figs 3–7). the planar cross section of a parallel sample was utilised in direction of the gradient and the location-dependence of the sphere diameters was calculated from the chord lengths, determined from micrographs.

[1]BAM = Federal Institute for Materials Research and Testing, Berlin.

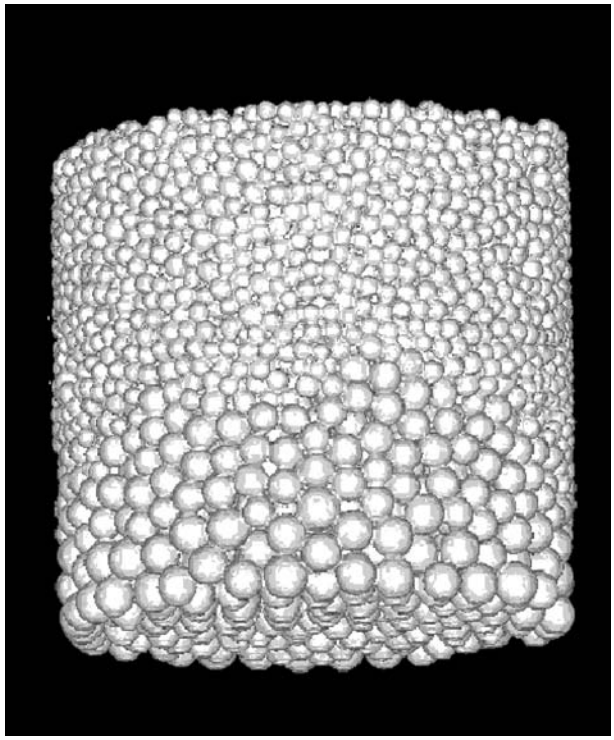

Figure 1 Isosurface representation of a ceramic filter sample.

3. Stereological analysis and determining gradient structures on the basis of cross sections

In image analysis in this investigation for the used stereological methods a trend-like variability of the microstructure in one principal direction (x-axis) is assumed, while vertically to the x-axis only random fluctuations, as are usually observable in a homogeneous structure, are allowed. Steep gradients are investigated showing a strong location dependence of the microstructural parameters. The aim is the determination of spatial pore and particle size distributions as well as the location-dependent stereological basic characteristics like volume fraction $V_V(x)$, particle density $N_V(x)$ and surface density $S_V(x)$. By means of lineal or area analysis, the stereological estimation for the location-dependence of volume fraction $V_V(x)$ is straightforward.

A method with no assumptions of particle shape was developed by Hahn et al. to evaluate the local surface density $S_V(x)$. Similarly it is possible to estimate the local length density to describe the gradient in fibre-reinforced materials. An extensive representation of these results is given in [9].

The determination of the spatial particle size frequency distribution using the measured data of the planar cross section needs the assumption of the particle shape. For homogenous microstructures with a random distribution of the microstructure parts calculations for various particle shapes can be already found in the literature [10–11].

Starting with the assumption of spherical particles or pores an evaluation method was developed enabling the

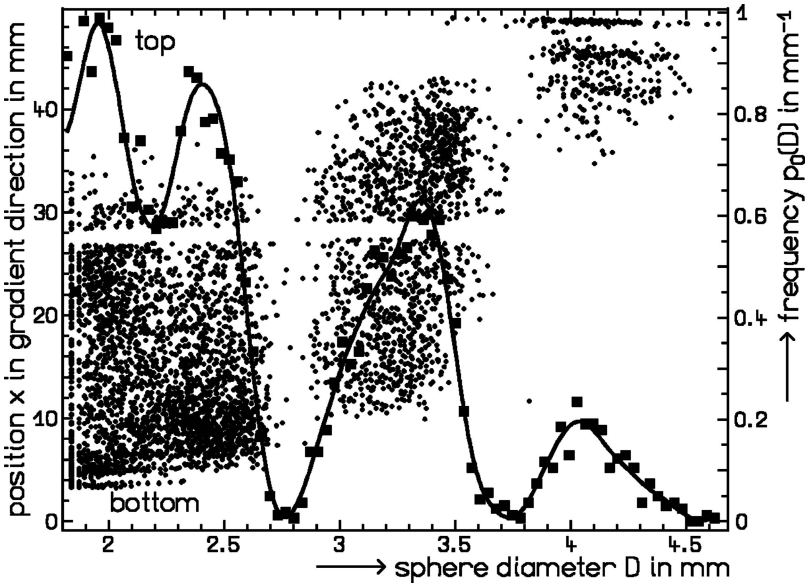

Figure 2 Global sphere diameter distribution of ceramic filter and locally resolved sphere diameter distribution. Each dot represents one sphere. The gap at a horizontal x-position of about 28 mm results from the fact that the used computer memory allowed only the analysis of half the data set at one time. Thus spheres which were not fully located in one half of the data set gave rise to artefacts in the plot.

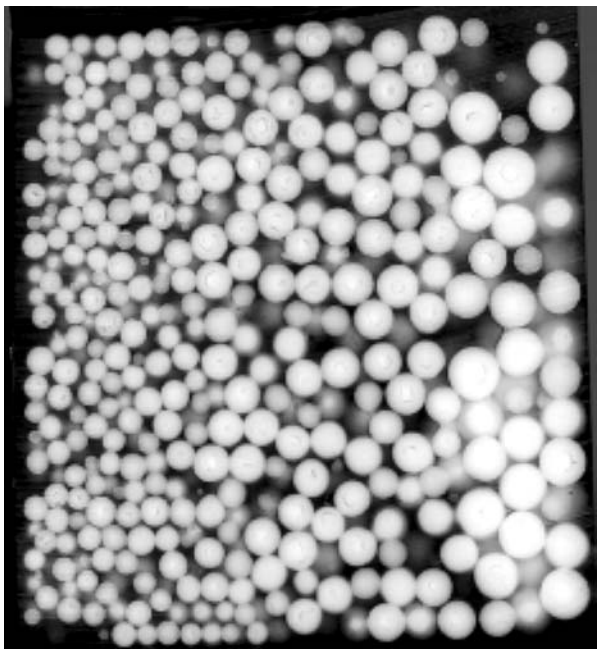

Figure 3 Cross section through the ceramic filter (left: top; right: bottom in Fig. 1).

calculation of the gradient of the spatial particle size using the measured chord lengths or circle diameters in the plane section in dependence of the local coordinate. The distribution of the spatial particle sizes (sphere diameters) is approximated by a lognormal distribution. There exists a very simple relation between the moments of the distributions of the sphere diameters, the circle diameters and the chord lengths for spheres.

This yields to simple formulae for the standard deviation $\sigma(x)$ and the peak position $D_0(x)$ of the sphere diameter distribution (see details in the appendix). The determination of the moments is straightforward. This method is a robust stereological procedure which also compensates errors in preparation to some extent.

Of course, the assumptions of a lognormal distribution and of spheres are certain drawbacks. However, because of using the moments, the results for other distributions than lognormal give at least good approximations for the average values (e.g. $D_{av}(x)$, $N_v(x)$, $S_v(x)$). The standard deviation $\sigma(x)$ is for this case only an effective measure for the width of the distribution function. Especially for narrow distributions it is only little dependent on the kind of the distribution.

The advantage of this procedure compared to the already known method by Hahn et al. [9] is the possibility not only to calculate the local dependence of the average sphere diameter, but also of the standard deviation of this value. This is especially of interest for a particle size distribution varying locally in width, e.g. in case of creating a gradient in the particle arrangement by centrifugal sedimentation, where in the beginning the total particle size distribution is present, while at the end only the smallest particles are settled.

The stereological methods both for $\sigma = f(x)$ and $\sigma = \text{const.}$, based on the moment method, were combined in one computer program (GRADIENT[2]), which uses chord lengths or equivalent circle diameters obtained by standard procedures of an image analysis system. In case of $\sigma = \text{const}$ the method similar to Hahn et al. [9] is used, determining a master frequency distribution, which is subsequently evaluated using three moments (with $n = 0$, 0.5, 1). With the developed computer program it is possible to line up several measuring

[2] A zero version could be obtained by the corresponding author.

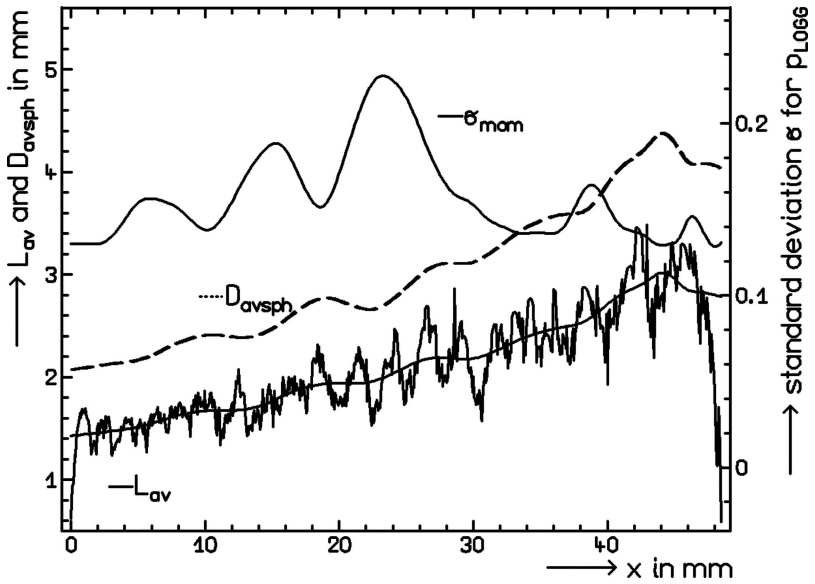

Figure 4 Local-dependence of L_{av}, D_{avsph} and σ_{mom} (method of moments) L_{av} = average chord length, D_{avsph} = average sphere diameter, σ_{mom} = standard deviation.

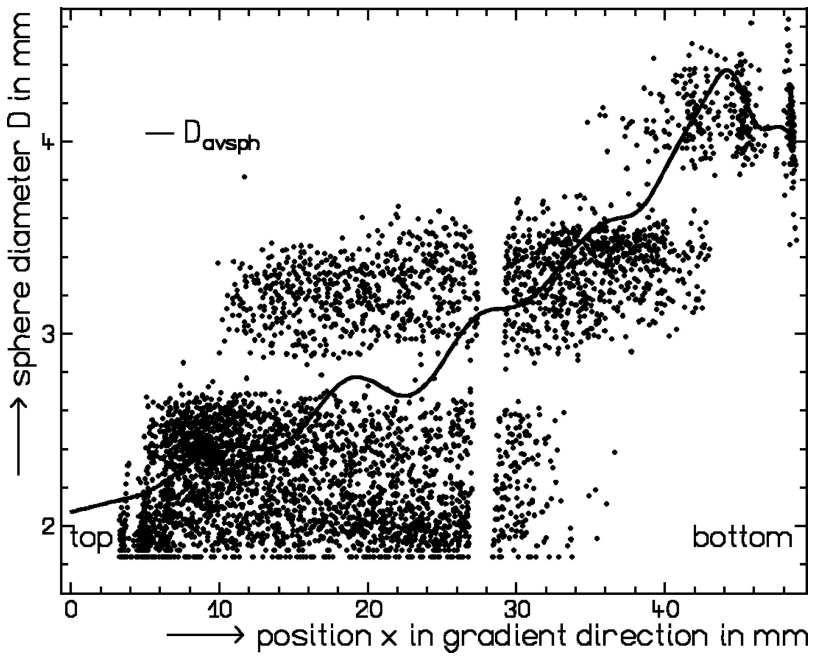

Figure 5 Comparison of the results of computed tomography (see Fig. 2) with D_{avsph} (Fig. 4) D_{avsph} = average sphere diameter.

fields with or without gaps. Intersection (overlapping) and changing calibration factors for the individual measuring fields are allowed as well. Additionally it is also possible to average over each single measuring field. This procedure was implemented also to characterise long range gradients.

With help of this program, starting from planar section, the following gradient characteristics, which are averaged over a definite number of measuring points (points in x-axis direction), can be determined:

$L_{av}(x)$, $\phi_{av}(x)$, $D_{av}(x)$, $\sigma(x)$, $N_V(x)$, $S_V(x)$, $V_V(x)$ and the cumulative (P) or frequency (p) logarithmic sphere diameter distributions of numbers (index 0) or volumes (index 3) (i.e. $V_V * p_3(\log D)$); "av" means averaging over the according frequency distributions belonging to one x-location (L_{av} = average chord length, ϕ_{av} = average circle diameter, D_{av} = average sphere diameter, $V_V(x)$ = volume fraction, $N_V(x)$ = particle density, $S_V(x)$ = surface density). The chord lengths (lineal analysis) and circle diameters (area analysis) are determined by image analysis. They represent the basic data for calculating the location-dependence. By means of automated evaluation procedures of the quantitative microstructure analysis a large number of data can be collected giving a sufficiently

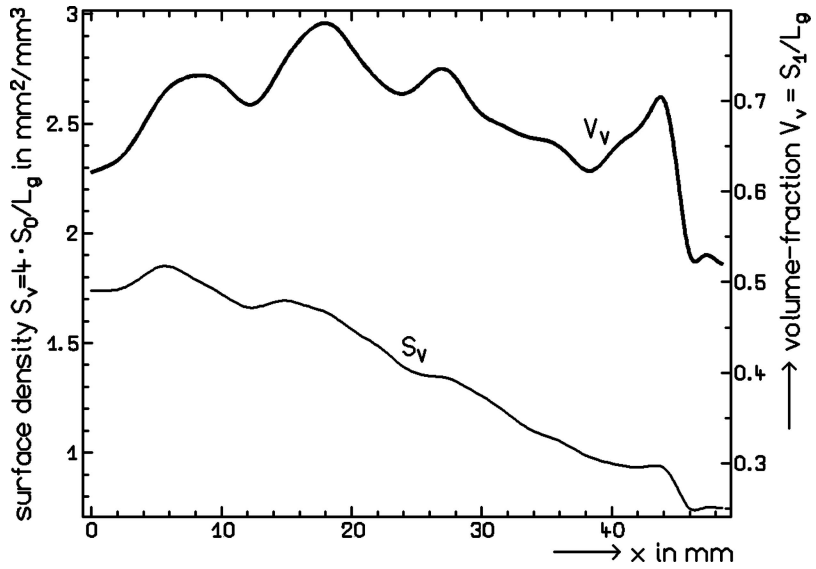

Figure 6 Local-dependence of S_V and V_V of spheres (method of moments) S_v = total surface/volume, V_v = volume fraction.

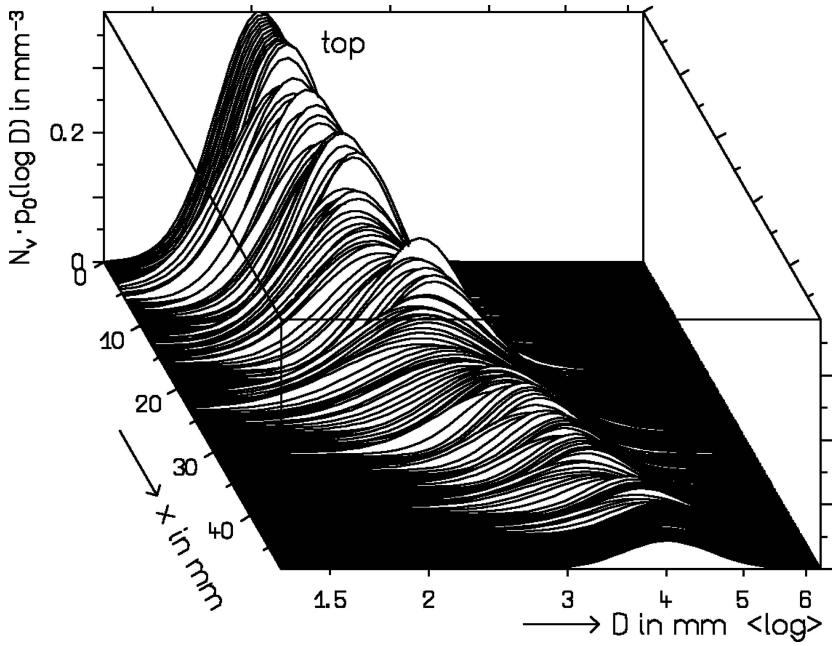

Figure 7 Local-dependence of number weighted frequency distribution of sphere diameters N_v = number of spheres/volume.

statistical accuracy for the calculation of the spatial diameter distribution.

A direct determination of the gradient of the spatial particle size distribution is only possible with CT. For comparison of the two methods, image analysis and CT, the same gradient filter as in section 2 was used. In this way it was possible to compare the CT-investigations with the calculations of the sphere diameters from the chord length data directly. Polished sections were prepared and investigated. Fig. 3. shows a planar section through the filter (for comparison see Fig. 1). Here the particle shape is spherical and the gradient of the particle sizes shows an almost monotonic behaviour (Fig. 4). For comparison with the results of CT the data of Fig. 2 are mirrored and plotted together with D_{avsph} from Fig. 4 in Fig. 5. The volume fraction of the particles is higher in the transition zones, since with a wider particle diameter distribution a better packing density of spheres is achieved (Fig. 6). Fig. 7 shows the number frequency distribution of particles. The local dependence of the distributions is in good agreement with the original five fractions. Of course due to the used evaluation method no bimodal distributions could be obtained. However, in the overlapping region a broadening of the frequency distributions can be observed. In spite of not lognormally distributed spheres, the tendencies can be shown clearly.

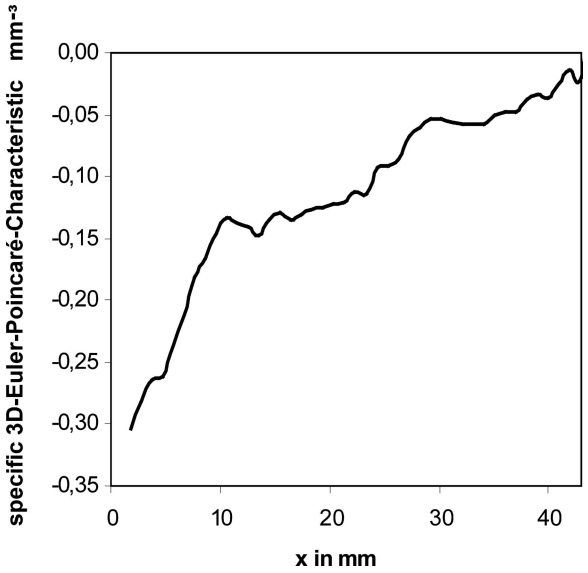

Figure 8 Location-dependence of the specific Euler-Poincaré–Characteristic $K_v(x)$ (from CT, left: top, right: bottom).

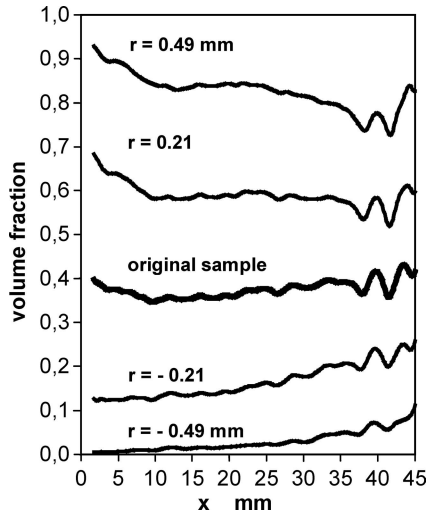

Figure 9 Effect of erosion ($r < 0$ mm) and dilation ($r > 0$ mm) of the location-dependence of the volume fraction (pore system) (from CT), r = radius of testing sphere.

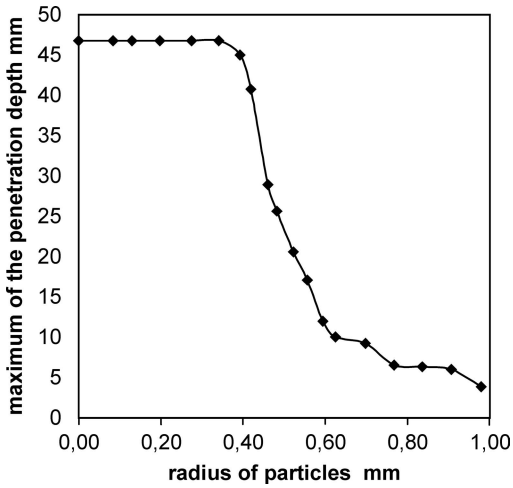

Figure 10 Maximum of the penetration depth d_p in dependence of the radius r of the testing sphere (from CT).

4. Characterisation of gradient structures by means of mathematical morphology

An alternative to the particle-based methods described in section 3 is to analyse the set X of all particles (or all pores) as a whole. The analysis consists in application of operations of mathematical morphology such as "dilation" and "erosion", see Ohser et al. [10] or Soille [12]. Erosion and dilation procedures consist of reducing or enlarging the particles or pores by a certain amount of a sphere radius r. Typically as structuring elements $b(0, r)$ disks or balls with a series of different radii are used. For the sets $X \oplus b(0, r)$ and $X \ominus b(0, r)$ the gradient-dependent volume fractions $V_V(x, r)$, (x = gradient variable, r = dilation radius if $r > 0$ and erosion radius if $r < 0$) can be valuable descriptors. For example, if for some regions of x-values the particles are small, then already for small negative values of r, $V_V(x, r)$ may be close to zero. So it is possible to find a particle size gradient without size measurement even in the case of constant volume fraction $V_V(x)$.

If three-dimensional data are given, in this example obtained by CT (see Section 2) for the same ceramic filter as with the other evaluations, mathematical-morphological operations can help to determine the penetration depth of spherical particles into porous structures without experiments with real particles. It suffices to erode the systems of pores by spheres and to study the connectivity of the resulting set.

Based on three-dimensional data also the location-dependent connectivity density (or specific Euler-Poincaré characteristic) $K_V(x)$ can be determined, see Ohser et al. [10]. (In 2D $K_v(x)$ is defined as the sum of interconnected components, e.g. in a binary image, minus the number of holes). The idea is to determine K_V for a layer located at x and orthogonal to the gradient, using the method described in [13].

Fig. 8 shows $K_V(x)$ for the three-dimensional gradient structure corresponding to the planar section given in Fig. 3. With increasing x one observes increasing values of $K_V(x)$. The negative values of $K_V(x)$ for small x correspond to a high degree of connectivity because of the big influence of sinter-necks. For big particles (at large x) the influence of the necks decreases and consequently the degree of connectivity is smaller.

Fig. 9 shows $V_V(x, r)$ for the system of pores in the structure corresponding to Fig. 3. It corresponds to three-dimensional data and erosion and dilation with spheres. The curve for $V_V(x) = V_V(x, 0)$ corresponding to the original pore system is nearly horizontal, indicating that there is no volume gradient. The dilated pore system (positive r) has a porosity decreasing in x, since the thin pores in

the dense system of small particles for small x are heavily enlarged by dilation. In contrast, the eroded pore system (negative r) has a porosity increasing in x, since the small pores vanish by erosion faster than the large pores at large x. Thus the morphological operations show in an indirect way the pore size gradient in the structure compared to Fig. 6, where directly the dependences for the particles are shown.

Fig. 10 shows the penetration depth (d_p) for the same structure, i.e. the maximal depth d_p attainable for a spherical particle of radius r if it starts in a pore on the side with the big particles (bottom). Clearly for very small spheres d_p is equal to the whole thickness of the sample, but for $r > 0.4$ mm d_p decreases, and it is close to 0 for $r = 1$ mm. This curve was obtained by eroding the three-dimensional pore system by a sphere of radius r.

5. Conclusion

This paper represented methods characterising gradient materials for one special example, a ceramic filter consisting of Al_2O_3-spheres. CT and image analysis on cross sections have been applied.

The results can be summarised as following:

- By means of computed tomography (CT) the spatial structure of materials could be evidenced directly. The measured data represent a base to calculate microstructural parameters such as volume fraction, particle and pore sizes. A universal application of this method is restricted up to now by the available resolution (approximately 2 μm).
- Statistical methods were developed calculating the location-dependence of spatial pore and particle size distributions. Planar sections (polished sections) through the materials in direction of the gradient and their image analysis yield the base for the statistical analysis. The investigations resulted in a computer program which allows the use of measuring data such as chord lengths (1D-lineal analysis), circle diameters (2D-area analysis) and equivalent sphere diameters (3D-CT or sphere projections). The determination of spatial particle size distributions is based on the assumption that the particles are spheres. The procedure was applied for the particular example of a ceramic filter. The results are in close correlation to the results from the 3D-analysis with CT.
- An alternative method for describing gradient structures is the use of techniques of mathematical morphology. In this way it is possible to characterise gradients without particle size measurements and to quantify the connectivity of pore systems. For this purpose it is necessary to apply methods of a 3D-image analysis. The necessary data can be obtained by means of CT. The application of this method was demonstrated for the gradient filter again.
- On the same gradient sample (the ceramic filter), the data from CT were also used to perform the mathematical morphology evaluation. Therefore it was possible, to compare the results of CT, mathematical morphology evaluation and the 2D-image analysis directly with one sample. The results turned out to be comparable very well. However, each method has its special advantages and disadvantages and enables the determination of different quantities, e.g. average values or distributions.
- Provided it is possible to get sufficiently accurate data either from CT or image analysis the demonstrated evaluation methods can be used for any kinds of functionally gradient materials with a gradient in one direction.

6. Appendix

When evaluating microstructures, frequency distributions can be determined by evaluating particle diameters (approximated as spheres, preferably directly determined with CT), or equivalent circle diameters or chord lengths with images on polished sections.

The moments of these distribution functions are very useful for further evaluations:

$$M_n = \int_{-\infty}^{\infty} D^n p_0(\ln D)\, d\ln D \qquad p_0 = \text{sphere diameter frequency distribution (probability density)} \qquad \overline{D} = \frac{M_1}{M_0} \tag{1}$$

$$R_n = \int_{-\infty}^{\infty} \phi^n q_0(\ln \phi) d\ln \phi \qquad q_0 = \text{circle diameter frequency distribution (probability density)} \qquad \overline{\phi} = \frac{R_1}{R_2} \tag{2}$$

$$S_n = \int_{-\infty}^{\infty} L^n s_0(\ln L) d\ln L \qquad s_0 = \text{circle diameter frequency distribution (probability density)} \qquad \overline{L} = \frac{S_1}{S_2} \tag{3}$$

$\overline{D}$, $\overline{\phi}$ and $\overline{L}$ are sphere average diameters, circle diameters or chord lengths respectively.

These moments satisfy the following general relations for spherical particles:

$$\frac{R_n}{R_0} = k_n \frac{M_{n+1}}{M_1} \tag{4}$$

$$\frac{S_n}{S_0} = k_n \frac{R_{n+1}}{R_1} = \frac{2}{n+2} \frac{M_{n+2}}{M_2} \tag{5}$$

$$k_n k_{n-1} = \frac{\pi}{2(n+1)} \quad k_0 = 1, n \geq -1 \tag{6}$$

The following stereological parameters can be obtained with these moments:

$$L_L = \frac{S_1}{L_t} = A_A = \frac{\pi}{4}\frac{R_2}{A_t} = V_V = \frac{\pi}{6}\frac{M_3}{V_t} \tag{7}$$

V_t = total volume, A_t = total area of evaluated image, L_t = total length of all evaluated lines. L_L = chord length fraction, A_A = area fraction, V_V = volume fraction

$$S_V = \pi \frac{S_0}{L_t} = 4\frac{R_1}{A_t} = \pi \frac{M_2}{V_t}, \; S_V = \text{surface/volume} \tag{8}$$

$$N_V = \frac{M_0}{V_t}, \; N_V = \text{numbers of particles/volume} \tag{9}$$

In addition also average particle sizes can be determined. However, in general, these evaluations, when using image analysis, are very inaccurate, because of not sufficient statistics, especially, when only very small ranges perpendicular to the gradient can be evaluated. Therefore the assumption of a special distribution function is useful, because then only two quantities must be determined (maximum position and width) to have a full description of the distribution function and all the related stereological parameters.

In our case lognormal distributions of sphere diameters are used:

$$p_0(\ln D) = p_{00} \exp\left(-\frac{\ln^2 D/D_0}{2\sigma^2}\right) \tag{10}$$

D_0 = peak position, σ = standard deviation, p_{00} = peak height.

For this distribution function the following relation holds:

$$M_n = D_0^n e^{n^2\sigma^2/2} M_0 \tag{11}$$

Using M_0, $M_{1/2}$, M_1 directly determined from 3D-measurements (sphere diameters, e.g. CT within small plates), or R_0, $R_{1/2}$, R_1 from 2D-measurements (circle diameters on polished sections within small strips) or S_0, $S_{1/2}$, S_1 from 1D-measurements (chord lengths on polished sections along lines) perpendicular to the x-direction σ and D_0 can be determined in dependence of x (using (11), (4), and (5)):

$$\sigma^2 = 4\ln\frac{M_0 M_1}{M_{1/2}^2} = 4\ln a\frac{R_0 R_1}{R_{1/2}^2} = 4\ln b\frac{S_0 S_1}{S_{1/2}^2}, \quad \text{with } a = 0.9726, \; b = 0.96 \tag{12}$$

$$D_0 = e^{-\sigma^2/2}\frac{M_1}{M_0} = \frac{4}{\pi}e^{-3\sigma^2/2}\frac{R_1}{R_0} = \frac{3}{2}e^{-5\sigma^2/2}\frac{S_1}{S_0} \tag{13}$$

Using (11), (4), and (5) also all necessary moments in the above formulae (7–9) can be calculated just from the experimentally obtained moments $M_0, M_{1/2}, M1$, or $R_0, R_{1/2}$, R_1, or S_0, $S_{1/2}$, S_1. These moments were chosen, because they can be determined with comparably high accuracy (in contrast to e.g. M_3 or R_2). Nevertheless, smoothing of all obtained quantities in x-direction is necessary (this has been done in the program GRADIENT).

Acknowledgements

We thank the Deutsche Forschungsgemeinschaft (DFG) as carrier of the German Functional Gradient Materials research program which supported this work.

We are grateful to our co-workers at BAM E. Jasiuniene and B. Illerhaus for developing algorithms for image analysis. Dr. K. Rudolph of TU Bergakademie Freiberg, Institute of Ceramic, Glass and Building Materials is acknowledged for the fabrication of the corundum filters.

References

1. A. BÖRNER, R. HERBIG, M. MANGLER and G. TOMANDL, *Mater. Sci. Forum* **308–311** (1999) 89.
2. T. MORITZ, G. WERNER, G. TOMANDL, M. MANGLER, H. EICHLER, U. LEMBKE and W. HAUFFE, Dresden, *Mater. Sci. Forum* **308–311** (1999) 884.
3. U. BIRTH, M. JOENSSON and B. KIEBACK, *Mater. Sci. Forum* **308–311** (1999) 766.
4. M. MANGLER, G. TOMANDL and W. GRÜNEWALD, ; *Prak. Met. Sonderband* **34** (2003) 443.
5. L. A. FELDKAMP, L. C. DAVIS and J. W. KRESS, "Practical cone-beam algorithm", *J. Opt. Soc. Amer.* **1** (1984) 612.
6. J. GOEBBELS, G. WEIDEMANN, R. DITTRICH, M. MANGLER, G. TOMANDL, *Ceram. Trans.* **129** (2002), 113.
7. M. JOENSSON, B. KIEBACK in: B. ILSCHNER, N. CHERADI (eds.), Proc. 3rd Int. Symp. on Structural & Graded Materials, Lausanne (1995) p. 33.
8. J. GOEBBELS, B. ILLERHAUS, G. WEIDEMANN, K. PISCHANG, in Proc. Functionally Graded Materials 1998, edited by W. A. KAYSSER (Trans Tech Publications, Switzerland 1999) p. 867.

9. U. HAHN, A. MICHELETTI, R. POHLINK, D. STOYAN and H. WENDROCK, *J. Microscopy* **195** (1999) 113.
10. J. OHSER and F. MÜCKLICH in Statistical Analysis of Microstructures in Material Science, edited by Vic Barnett (John Wiley & Sons, LTD, Chister, 2000).
11. G. TOMANDL, M. MANGLER, E. PIPPEL and J. WOLTERSDORF, *Mater. Chemi. Phys.* **63** (2000) 139.
12. P. SOILLE, Morphological Image Analysis (Springer-Verlag, Heidelberg 1999).
13. W. NAGEL, J. OHSER, K. PISCHANG, *J. Microscopy* **198** (2000) 54.

Received 2 August
and accepted 8 September 2005